

See discussions, stats, and author profiles for this publication at: <https://www.researchgate.net/publication/231290685>

Secondary Formation and the Smoky Mountain Organic Aerosol: An Examination of Aerosol Polarity and Functional Group Composition During SEAVS

ARTICLE in ENVIRONMENTAL SCIENCE AND TECHNOLOGY · JANUARY 1998

Impact Factor: 5.33 · DOI: 10.1021/es970405s

CITATIONS

108

READS

33

6 AUTHORS, INCLUDING:



James D Blando

Old Dominion University

29 PUBLICATIONS 527 CITATIONS

SEE PROFILE



Robert Porcja

Rutgers, The State University of New Jersey

10 PUBLICATIONS 630 CITATIONS

SEE PROFILE



Paul J Liroy

Environmental and Occupational Health Scie...

368 PUBLICATIONS 8,982 CITATIONS

SEE PROFILE

Secondary Formation and the Smoky Mountain Organic Aerosol: An Examination of Aerosol Polarity and Functional Group Composition During SEAVS

JAMES D. BLANDO, ROBERT J. PORCJA, TSUNG-HUNG LI, DAVID BOWMAN, PAUL J. LIOY,[†] AND BARBARA J. TURPIN*

Department of Environmental Sciences and Rutgers Cooperative Extension, Rutgers University, ENRS Building, 14 College Farm Road, New Brunswick, New Jersey 08901-8551

Size-resolved particle samples were collected in the Smoky Mountains at Look Rock, TN, during the Southeastern Aerosol and Visibility Study (SEAVS) July–August 1995 and analyzed directly by Fourier transform infrared (FTIR) spectroscopy for functional group and chemical bond information. Twenty-eight samples were also gently rinsed in hexane, acetone, and water and reanalyzed after each rinse. Direct FTIR analyses of substrates rinsed with solvents enabled separation by polarity and identification of sulfur-containing organics even though samples were too small for traditional extraction and analysis (approximately 10–15 μg). The submicron organic aerosol was predominantly polar. Most of the nonpolar material, including aliphatic carbon and various minerals, was concentrated in particles greater than 1.0 μm and is most likely from primary biogenic and geogenic emissions, such as plant waxes and windblown soil dust. Unlike Los Angeles, carbonyl size distributions were unimodal and usually peaked in the 0.5–1.0 μm diameter size range. The predominance of sulfate, carbonyl, and organosulfur absorbances, the polarity of the aerosol, and the carbonyl size distributions indicate that secondary formation processes have a large influence on the concentrations, composition, and size distributions of the Smoky Mountain aerosol.

Introduction

Many researchers have shown that the polarity of organic aerosols influences environmental impacts of airborne particulate matter. Saxena et al. (1) found that near the Grand Canyon, a nonurban location, the presence of organics increased aerosol water uptake beyond that predicted for the particles' inorganic constituents. Conversely, the presence of organics in the Los Angeles urban aerosol decreased or retarded water uptake. To the extent that the nonurban Grand Canyon aerosol was the receptor of aged pollutants, it was likely to be more highly oxygenated and thus more polar and more hygroscopic than the fresh urban aerosol. Laboratory studies have also demonstrated that the presence of sorbed organic vapors can alter the water uptake of

deliquescent aerosols (2, 3). Aerosol hygroscopicity impacts visibility, cloud formation, radiative forcing, aqueous-phase chemistry, and the atmospheric removal of particle-phase compounds. Aqueous-phase oxidation of sulfur dioxide can be inhibited by the presence of organic surfactants, which form a surface film that affects the mass transport of gaseous species into the droplet (4). In addition, the polarity of the organic fraction of ambient particles has been shown to affect the mutagenicity of the aerosol (5, 6).

Organic particulate matter and particle precursors are emitted from a multitude of anthropogenic and biogenic sources. Roughly, 20–70% of the total dry fine particle mass is organic (7–9), and the organic fraction contains a large number and variety of compounds (10). Its composition and concentration exhibit strong diurnal and seasonal variability. Some organic compounds are emitted in the particle phase (i.e., primary aerosols). For example, *n*-alkane and *n*-alkanoic acids have primary sources such as epicuticular plant waxes, fungi, spores, pollen, algae, bacterial and fungal detritus, cooking, fossil fuel combustion, and biomass combustion (11). Atmospheric oxidation of gaseous organic emissions can yield low volatility products which form new particles or condense on preexisting particles. This process is called secondary organic aerosol formation, and tends to yield more highly oxygenated compounds, such as dicarboxylic acids. In both urban and more remote areas oxalic, malonic, succinic, and glutaric acids have been identified as the most prevalent dicarboxylic acids (11–13). Organic aerosol composition is also altered by changes in atmospheric conditions (i.e., temperature, humidity, and gas-phase concentrations) which drive the partitioning of semivolatile compounds between gas and particle phases (14, 15).

Gas chromatography/mass spectroscopy (GC/MS) provides quantitative analyses of individual compounds, but has only been able to identify a small fraction (typically 10–15%) of the organic aerosol mass (11). Organic aerosol characterization has relied heavily on gas chromatographic separation. Since the more polar compounds do not elute without modification (i.e. derivitization), our knowledge of organic aerosol composition is heavily weighted toward the less polar compounds. Fourier transform infrared (FTIR) spectroscopy is capable of characterizing a larger fraction of the sample mass, yielding functional group and bond information. Although FTIR does not provide individual compound identification, measurements can be made directly from particle samples without extraction or other sample processing, and analyses are nondestructive. For this reason, we were able to sequentially remove nonpolar organics, polar organics, and inorganic salts and obtain difference spectra of these ambient aerosol fractions even though loadings were much too small for identification using traditional extraction and analysis techniques (approximately 10–15 μg). The chemical information provided by this relatively quick and inexpensive technique can be used to optimize more detailed and costly analyses such as gas chromatography/mass spectroscopy to improve the fraction of organic mass identified at the molecular level.

FTIR spectroscopy has been used to study the sources and size distributions of aliphatics, carbonyls, and organonitrates in Los Angeles (16, 17), and the formation of secondary organics in smog chamber experiments (18). Gundel et al. (19) examined spectra of New Jersey particulate material extracted in cyclohexane, dichloromethane, and acetone and pressed into KBr pellets in a study of the composition, polarity, and mutagenicity of that aerosol. Grader et al. (20) used FTIR microscopy to study single

* To whom correspondence should be addressed: e-mail: Turpin@aesop.rutgers.edu; phone: 732-932-9540; Fax: 732-932-8644.

[†] Environmental and Occupational Health Sciences Institute, 681 Frelinghuysen Rd., Piscataway, NJ 08855.

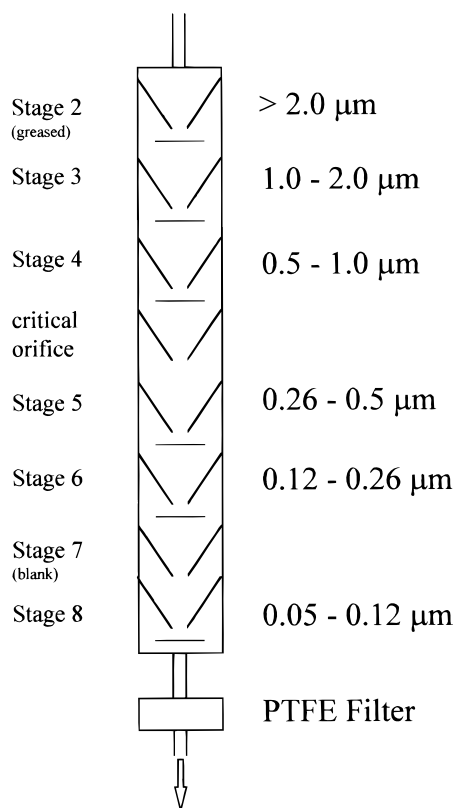


FIGURE 1. Schematic of Hering low-pressure impactor as used in this study, showing particle size fractions collected on each stage. A stretched Teflon filter collected particles smaller than 0.05 μm .

aqueous ammonium sulfate particles generated in the laboratory and suspended in an electrodynamic balance. Diffuse reflectance FTIR has been used to examine organic extracts fractionated by high performance liquid chromatography (21) and for real-time monitoring of heterogeneous reactions on artificial sea salt particles (22–24). The purpose of this study is to examine the composition, polarity, and sources (i.e., primary vs secondary) of the humid southeastern aerosol. This information is needed to understand particle properties and effects, and is essential to the evolution of predictive fine particle models that have primarily been tested with field measurements made in the arid southwest.

Experimental Section

Size-segregated samples were collected for functional group analysis as part of the Southeastern Aerosol and Visibility Study (SEAVS) at Look Rock in the Smoky Mountains (July 15–August 25, 1995). SEAVS was designed to improve simulation methods needed to assess the relationship between emissions, particle concentrations, and visibility in the eastern United States. An important focus of this work was the effect of organics on particle water content. An overview of the study is presented by Saxena and Musarra (25).

Each size-segregated Look Rock sample was collected from 0700 to 1900 eastern daylight time (EDT) on two consecutive days on zinc selenide (ZnSe) disks in a Hering Low-Pressure Impactor (LPI) (26, 27). Twelve-hour daytime collection periods were used by all investigators. A schematic of the LPI, including the size fractions collected on each stage, is shown in Figure 1. LPI stage 2 held a stainless steel disk coated with Apiezon N low vapor pressure vacuum grease to remove particles larger than 2.0 μm . LPI stages 3–6 and stage 8 held ZnSe disks, and a 25-mm stretched Teflon filter was placed downstream of the LPI to collect particles smaller

TABLE 1. Characteristic Wave Numbers of Functional Groups

functionality	approximate absorbance maxima (cm^{-1}) (28, 33)
sulfate ions (SO_4^{2-})	612–615, 1103–1135
bisulfate ions (HSO_4^-)	580–590, 867, 1029, 1180
ammonium ions (NH_4^+)	1410–1445, 3030–3052, 3170–3200
particle water ($-\text{OH}$)	1623, 3350–3450
aliphatic carbon ($\text{C}-\text{H}$)	2850–3000
carbonyl ($\text{C}=\text{O}$)	1640–1850
organonitrates (RONO_2)	856, 1278, 1631
alcohols (ROH)	3500–3750
alkene/aromatic carbon ($\text{C}=\text{C}$)	3000–3100
nitrate (NO_3^-)	830, 1340–1410, 1790
soil dust	540, 915, 1035, 3640

than 0.05 μm . Air was drawn through the system at 1.0 l/min, and pump exhaust was filtered with a Balston cartridge filter followed by a Gelman HEPA filter.

Substrates were loaded in the sampler (Figure 1) at a clean location within the main trailer. The sampler was checked for leaks, and the flow rate was measured at the beginning and end of each sampling period. The LPI flow rate was accurate within 2% as verified by an independent field auditor. After the first 12 h of sampling (0700 EDT, day 1) the pump was turned off. ZnSe substrates were left in the impactor awaiting the second 12-h collection period from 0700 to 1900 EDT on day 2. This was done to minimize sample handling while maintaining the same collection times as other SEAVS investigators. When the 24-h sampling period was complete, the substrates were removed from the impactor and placed immediately in substrate holders (plastic filter cassettes). ZnSe substrates are held firmly in filter cassettes so that the deposit is not disturbed during transit. Substrate holders were sealed with Teflon tape, wrapped in aluminum foil, placed in a Ziploc freezer bag, and stored in a freezer. They were then shipped back to the Environmental and Occupational Health Sciences Institute (EOHSI) with blanks via Priority Next-Day Air in coolers equipped with temperature recorders to measure the maximum and minimum temperature during shipment. Most SEAVS shipments remained below freezing and none exceeded 10 $^\circ\text{C}$ during transport to EOHSI in Piscataway, NJ. Samples were stored at -20°C and analyzed within 2–3 days of collection. They were allowed to equilibrate to room temperature just prior to sample analysis, which minimized condensation of water on the cold substrate.

Samples were first analyzed directly, without extraction, for functional group and bond information using a Mattson Research Series 100 FTIR Spectrometer located in the National Institute of Environmental Health Sciences Center of Excellence at EOHSI. Blanks and polystyrene standards were also analyzed using FTIR. The spectrometer has a deuterated triglycine sulfate (DTGS) detector. Energy throughput was typically 5.6 V. Samples were masked to minimize nonincident IR radiation and maximize spectrometer sensitivity. Masks of three different sizes (i.e., 1, 2, and 4 mm in diameter) were used to accommodate the various sample deposits, which ranged in size from 0.5–3.0 mm in diameter. Spectra of a clean area of the ZnSe substrate (background) and of the deposit (sample) were taken, and spectral results were presented as the percent of incident light absorbed versus wavenumber. Each spectrum is the average of 250 spectral scans at 4 cm^{-1} resolution. Functional groups were identified based on spectral libraries and standards (Table 1). Instrumental sensitivity was evaluated regularly by analyzing a standard thickness polystyrene film supplied by ATI Mattson (ATI Mattson, Madison, WI).

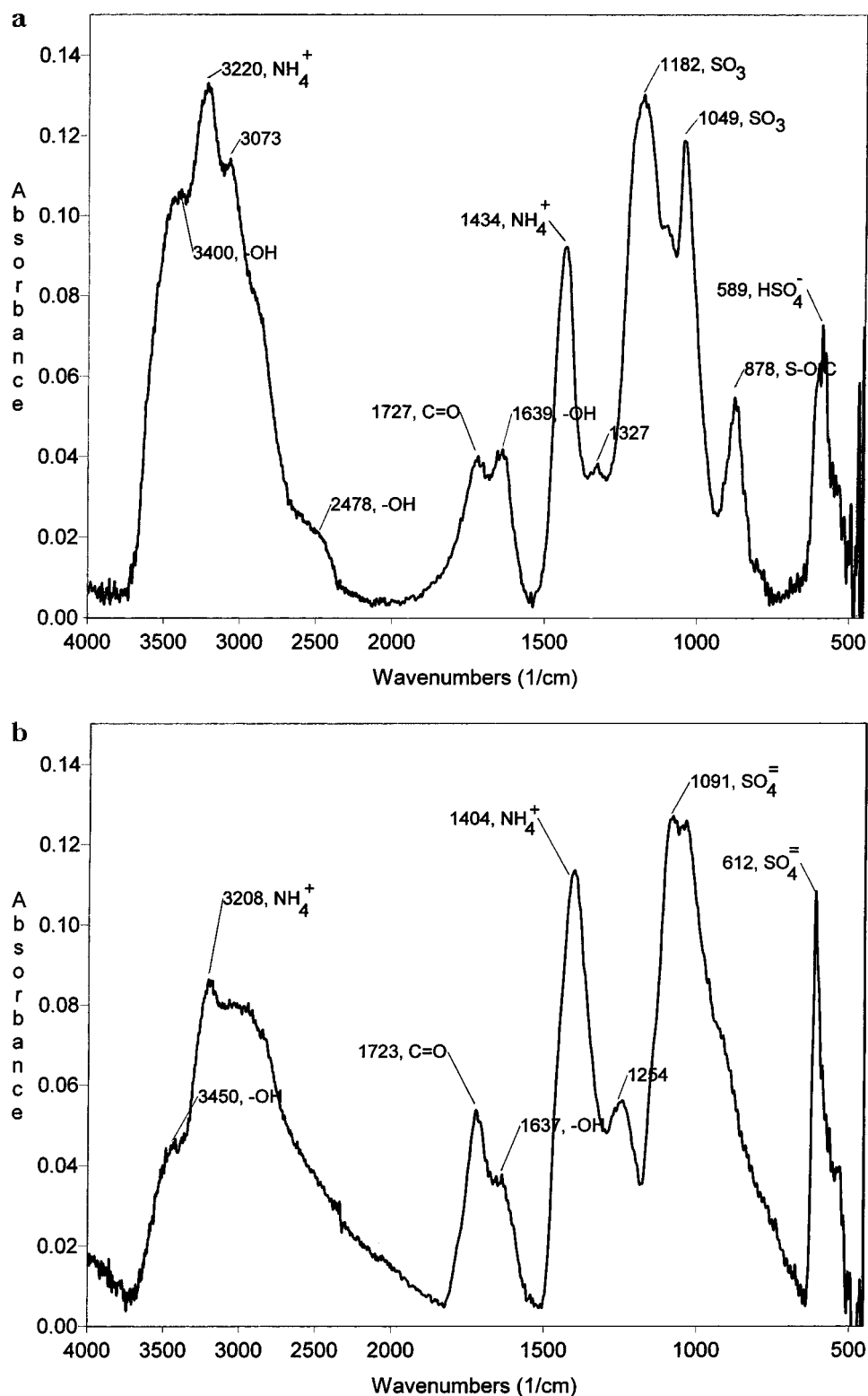


FIGURE 2. Fourier transform infrared (FTIR) spectra of 0.5–1.0 μm particles collected on August 13 (a) and July 25 (b), 1995 at Look Rock, Smoky Mountains, Tennessee. Labels indicate the centers of absorbance bands in wavenumbers.

Polystyrene peaks at 2979, 1621, and 799 cm^{-1} were integrated, and the variation in the absorbance of each peak was less than 0.3% over the course of the study.

Following initial analysis, we gently rinsed 28 samples collected August 13–24 in hexane, acetone, and water. The samples were reanalyzed after each rinse. Approximately 1 ml of solvent was drawn into a disposable pipet, and the substrate was held at a 45° angle. The solvent was applied above the deposit and allowed to flow slowly over the deposit

for approximately 5–10 s. This process was repeated twice. After each rinse the deposit was visually inspected to check for any sign of obvious particle disturbance. The substrates were air-dried at ambient temperature. Acetone was applied to the sample after the final water rinse to facilitate drying. Spectral-grade hexane, spectral-grade acetone, and deionized water were used in solvent rinses. The spectral simplification provided by the rinses was crucial to identification of important organic and inorganic constituents in the Smoky

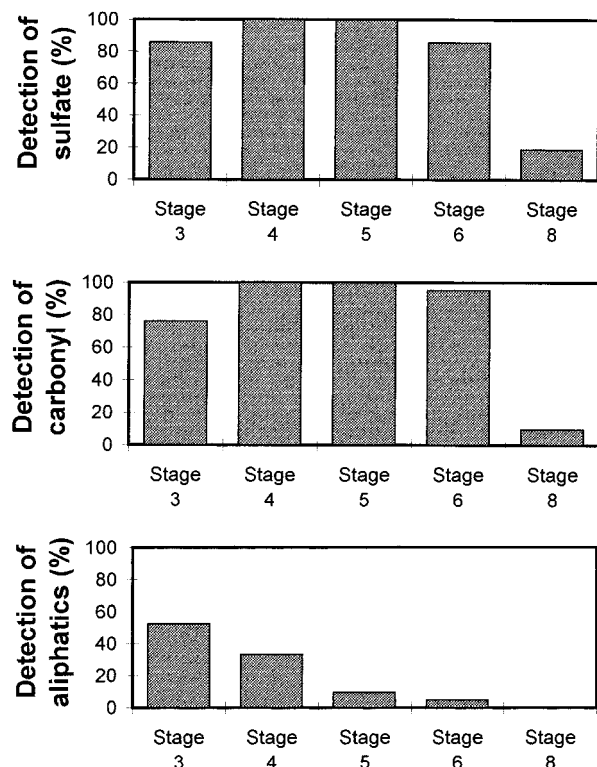


FIGURE 3. Frequency of detection of sulfate (a), carbonyl (b), and aliphatic absorbances (c) by stage (i.e., particle size fraction) based on 105 samples. Stage 3 collects 1.0–2.0 μm particles, stage 4 collected 0.5–1.0 μm particles, stage 5 collects 0.26–0.5 μm particles, stage 6 collects 0.12–0.26 μm particles and stage 8 collects 0.05–0.12 μm particles. Frequency is expressed as a percentage.

Mountain aerosol. The hexane rinse removes absorbances associated with nonpolar organic constituents, and absorbances removed with the acetone rinse describe the polar organic constituents. Water-soluble inorganic constituents, such as sulfate and nitrate, are removed in the water rinse. The final spectrum contains only insoluble constituents, such as soil dust.

After all analyses were complete, substrates were cleaned, analyzed, and returned to the field. An infrared analysis of cleaned substrates served as a performance check of substrate quality and ensured that contaminated substrates were not sent back to the field. In addition, every sample set had one field blank which was handled and transported in the same manner as the actual samples. Analyses of field blanks showed that none of the sample sets became contaminated during transport or storage.

To provide information on the performance of the technique, the same hexane, acetone, and water rinse procedure was applied to laboratory-generated aerosol standards of known composition, collected on ZnSe substrates in the LPI. Solvent rinses were performed on ammonium bisulfate aerosol samples and mixtures of ammonium sulfate and a single carbonyl-containing compound (i.e., oxalic, tartaric, glutaric, and adipic acid). These aerosols were generated in a Collision nebulizer, dried in a diffusion drier, collected in the LPI and analyzed before and after hexane, acetone and water rinses. Dynamic blanks were prepared by sampling the output of the aerosol generation system when only deionized water was atomized. Ten blank ZnSe substrates were also rinsed with solvents and analyzed in the same manner as the samples.

Results

Spectra of fine particle samples from the Smoky Mountains (e.g., Figure 2) contained strong sulfate/bisulfate and carbonyl

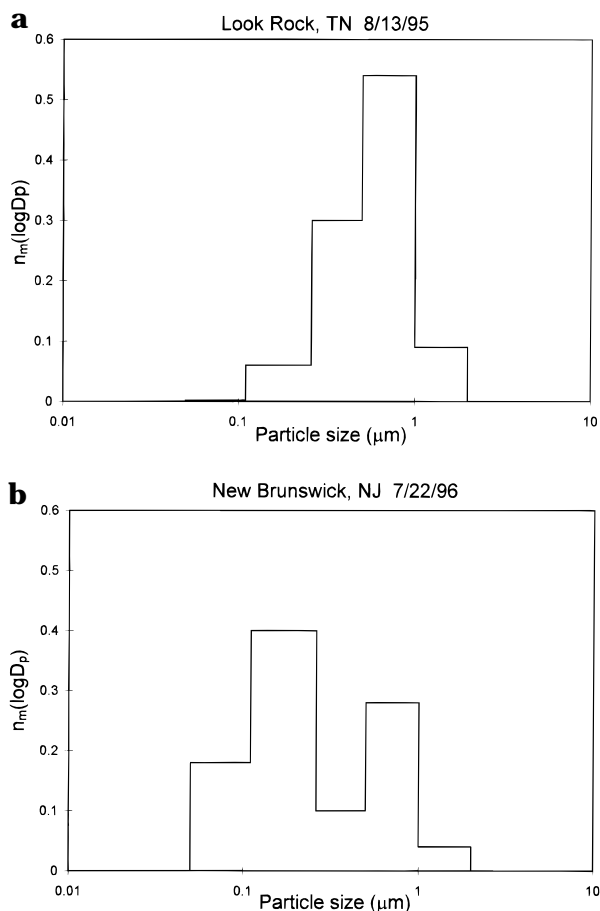


FIGURE 4. Carbonyl size distribution (normalized) for August 13–14, 1995, at Look Rock, Smoky Mountains, TN (a) and for July 22–23, 1996, in New Brunswick, NJ (b).

absorbances, like spectra of Los Angeles particles (16, 17, 28). Ammonium nitrate, which was an important constituent in Los Angeles, was not detected in the FTIR spectra of Smoky Mountain aerosol. This finding is consistent with the nitrate and nitric acid measurements of other SEAVS investigators and thermodynamic equilibrium model calculations that predict that the nitrate at Look Rock during the study is almost entirely in the gas phase (25). The size distributions of aliphatic and carbonyl carbon differed dramatically from the Los Angeles aerosol. The frequency of detection of sulfate, carbonyl, and aliphatic carbon as a function of particle size is shown in Figure 3. Sulfate and carbonyl absorbances were found on all stages but were frequently below detection limits on stage 8 (0.05–0.12 μm diameter particles). In contrast, aliphatic absorbances were quite small and were most frequently detected in 1.0–2.0 μm particles (stage 3).

Figure 2 shows spectra of 0.5–1.0 μm particles collected on August 13–14 (a) and July 25–26 (b), 1995. A broad, high-frequency absorbance band is typically present and includes hydroxyl (e.g., water), ammonium, aliphatic, and aromatic absorbances. Absorbances for carbonyl and hydroxyl between 1600 and 1800 cm^{-1} overlap, but are easily separated with peak-resolution software. The July 25–26 spectrum contains sulfate, which absorbs at 612 cm^{-1} , whereas the August 13 spectrum contains bisulfate. The incomplete neutralization of sulfate is consistent with other data from the eastern United States (29, 30). It should be noted, however, that we took no special precautions to prevent the neutralization of acidic sulfate by ammonia during sample handling. The FTIR NH_4/SO_4 absorbance ratios are reasonably well correlated ($R^2 = 60\%$) with Harvard HEADS NH_4/SO_4 molar ratios during the later part of the

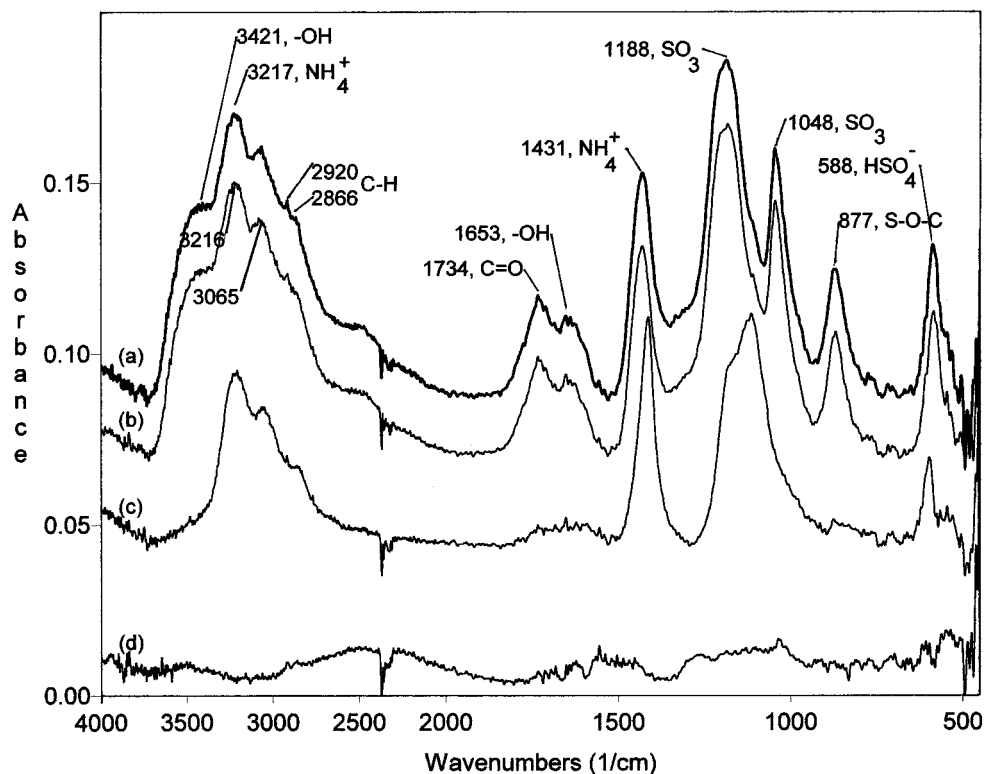


FIGURE 5. FTIR spectra of 0.5–1.0 μm diameter particles collected on August 21–22, 1995, at Look Rock, Smoky Mountains, TN. Shown are the original spectrum (a), the spectrum after removing nonpolar organics with hexane (b), the spectrum after subsequent removal of polar organics in acetone (c), and the spectrum after subsequent removal of inorganic salts in water (d). Several absorbances are labeled with functional group assignments and with absorbance bands in wavenumbers.

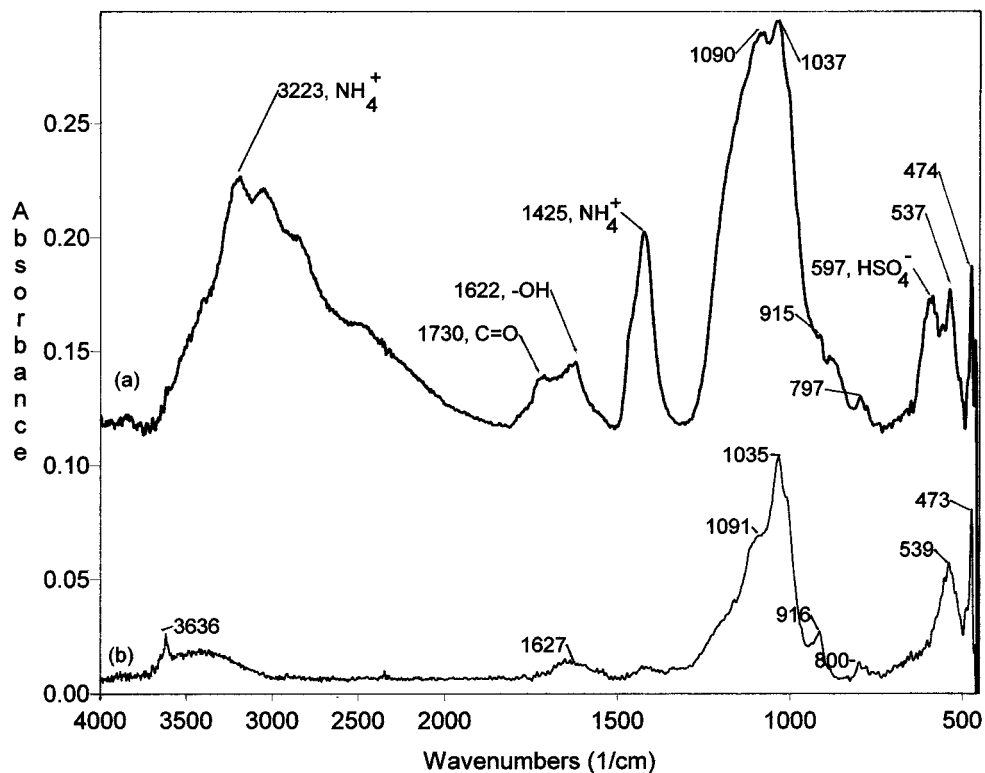


FIGURE 6. Spectra of 1.0–2.0 μm particles collected on August 17–18, 1995, at Look Rock, Smoky Mountains, TN. Shown are the original spectrum (a) and the spectrum after gentle rinsing with hexane, acetone, and water (b). Several absorbances are labeled with functional group assignments and with absorbance bands in cm^{-1} . Absorbances at 539, 800, 916, 1035, 1091, and 3636 wavenumbers are characteristic of clay-like soil dust.

study (August 10–25) when particle concentrations were high and NH_4/SO_4 molar ratios were low. Poor correlations were

found earlier in the study, when the air mass was relatively clean. This suggests that direct FTIR analysis of aerosol

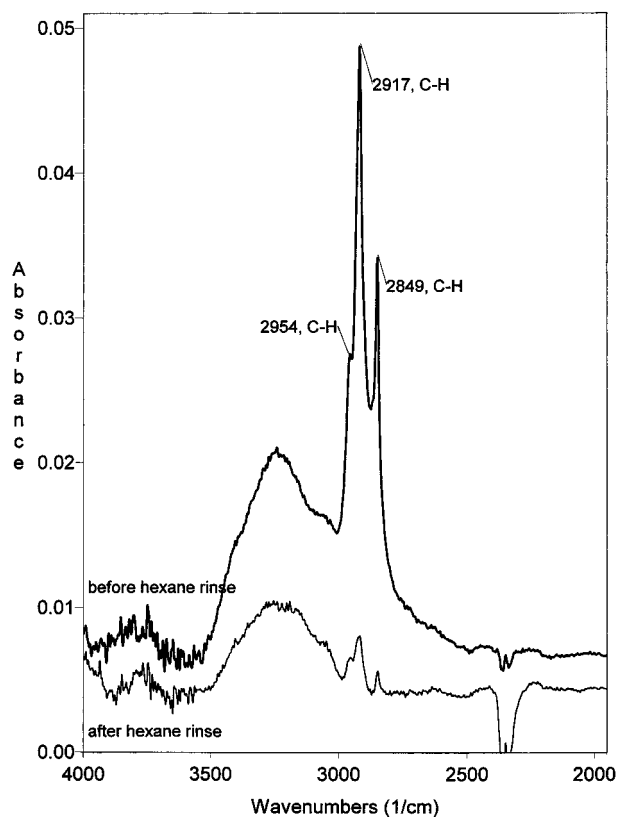


FIGURE 7. Aliphatic region of a sample collected in a cigarette smoke-impacted residence. Shown are the original spectrum (a), and the spectrum after removing nonpolar organics with hexane (b). Several absorbances are labeled with absorbance bands in wavenumbers.

deposits has the potential, with proper precautions, to provide size-resolved information concerning sulfate acidity.

Carbonyl and Aliphatic Size Distributions. The occurrence and size distribution of aliphatic carbon at Look Rock were distinctly different from those of the Los Angeles aerosol. Aliphatic carbon absorbances in Los Angeles spectra were much more substantial than aliphatic absorbances in the Look Rock spectra. In addition, size distributions of Los Angeles aliphatic carbon peaked at $0.076\text{--}0.12\text{ }\mu\text{m}$ (16), whereas aliphatics in the Look Rock aerosol were most prevalent in $1.0\text{--}2.0\text{ }\mu\text{m}$ diameter particles (see Figure 3). In Los Angeles, aliphatic carbon was attributed to primary automotive emissions. Aliphatics in the $1.0\text{--}2.0\text{ }\mu\text{m}$ size fraction at Look Rock are likely to represent the lower tail of a "mechanically derived" aerosol. Considering the proximity of the sampling site to vegetative sources, the aliphatics are probably of primary biogenic origin, e.g., plant waxes (31).

Figure 4 shows the normalized carbonyl size distribution for August 13–14, 1995, at Look Rock (a) and July 22–23, 1996, near the Photochemical Assessment Monitoring Site, New Brunswick, NJ (b). Carbonyl and sulfate peaks were resolved from neighboring peaks and integrated using GRAMS/32 peak resolution software (Galactic Industries Corporation, Salem, NH). Carbonyl size distributions for samples collected in the Smoky Mountains were unimodal with a peak in the $0.5\text{--}1.0\text{ }\mu\text{m}$ diameter size fraction, or occasionally in the $0.26\text{--}0.5\text{ }\mu\text{m}$ size fraction, as shown in Figure 4a. The only two exceptions were samples collected on August 3–4 and August 21–22, which had bimodal distributions. Smoky Mountain carbonyl size distributions are distinctly different from those observed in the Los Angeles Basin. Most carbonyl size distributions measured in the Los Angeles Basin (16) were bimodal with peaks near $0.12\text{--}0.26$

μm and $0.5\text{--}1.0\text{ }\mu\text{m}$ in diameter like the New Brunswick, NJ, sample shown in Figure 4b.

It is generally accepted that the major source of particulate carbonyl carbon is photochemical oxidation of gas-phase hydrocarbons of anthropogenic and biogenic origin (32). Particle-phase carbonyl carbon is also emitted from vehicular and biogenic sources. Pickle et al. (16) estimated that greater than 90–95% of the carbonyl carbon measured in Los Angeles was secondary organic aerosol. Source measurements of vehicular emissions in the Caldecott tunnel made by Pickle et al. (16) show that carbonyl carbon emitted by motor vehicles is confined to $0.075\text{--}0.26\text{ }\mu\text{m}$ particles, and the ratio of primary vehicular carbonyl to aliphatic carbon in similarly sized particles is 0.2:0.5. Aliphatic carbon absorbances in particles less than $0.26\text{ }\mu\text{m}$ in diameter are quite small in the Smoky Mountain aerosol, and size distributions of Smoky Mountain carbonyl do not exhibit a peak below $0.26\text{ }\mu\text{m}$. Therefore, primary motor vehicle emissions cannot account for the carbonyl carbon measured in the Smoky Mountains. Because primary biogenic particles are mechanically derived, primary biogenic emissions would generate coarse-mode carbonyl. Thus, primary biogenic emissions cannot explain the $0.5\text{--}1.0\text{ }\mu\text{m}$ carbonyl peak. For these reasons, the contribution of secondary carbonyl carbon to the fine aerosol appears to be large relative to primary carbonyl from local biogenic sources and motor vehicles. The predominance of sulfate and carbonyl absorbances in the Smoky Mountain spectra underscores the importance of secondary formation mechanisms in the southeastern fine aerosol.

Solvent Rinses. Selective solvent rinses coupled with FTIR analysis show that the Smoky Mountain aerosol is predominantly polar. Figure 5 shows the original infrared spectrum of $0.5\text{--}1.0\text{ }\mu\text{m}$ diameter particles collected August 21–22 and the spectra collected after the sample was rinsed with hexane, acetone, and finally water. Table 2 summarizes the results of solvent rinses. Rinsing SEAVS submicron samples in hexane to remove nonpolar organics resulted in little or no spectral change. When these same samples were rinsed in acetone to remove polar organics, several large peaks were removed, indicating that a large fraction of the organic aerosol is polar. Spectral subtraction verified that peaks at approximately 875 , 1045 , and 1225 cm^{-1} were present in 10 of the 28 samples rinsed, and in all cases, these peaks were removed with the acetone rinse. Frequently, a small broad peak at approximately $2490\text{--}2500\text{ cm}^{-1}$ was present and removed in acetone. The acetone rinse also removed submicron carbonyl (approximately 1730 cm^{-1}) and hydroxyl (1630 , 3450 cm^{-1}) in all stage 4–8 samples. Five of the six stage 3 samples ($1.0\text{--}2.0\text{ }\mu\text{m}$ diameter particles) appeared to contain a carbonyl absorbance, poorly separated from the neighboring hydroxyl absorbance, that was removed in water rather than in acetone. This suggests that carbonyl carbon in the $1.0\text{--}2.0\text{ }\mu\text{m}$ size fraction was somewhat different than the submicron carbonyl.

After polar organics were removed in acetone, inorganic salts (i.e., sulfates) were removed by rinsing samples gently with deionized water. As shown in Table 2, ammonium and sulfate absorbances were always removed in the water rinse. This left no detectable absorbances on submicron samples, and yielded a clear soil dust signature on supermicron ($1.0\text{--}2.0\text{ }\mu\text{m}$) particle samples. Figure 6 shows spectra of supermicron ($1.0\text{--}2.0\text{ }\mu\text{m}$) particles collected on August 17–18, 1995, prior to any rinses and after rinsing in hexane, acetone, and water. The post water-rinse spectrum is consistent with a large number of published spectra of minerals of the kaolinite and serpentine varieties with peaks at approximately 540 , 800 , 915 , 1035 (with shoulders), and 3640 cm^{-1} (33). With the exception of 540 cm^{-1} , these peaks are obscured by sulfate/bisulfate in the original spectrum, but the soil dust signature is quite evident after the final rinse. Absorbances

TABLE 2. Results of Solvent Rinses^a

	August Date					
	stage					
	13-14*	15-16*	17-18	19-20	21-22	23-24
	34568	34568	34568	34568	34568	34568
wavenumber range						
580-620 (sulfate/bisulfate)	wwwww	xwwwx	wwwww	wwwwx	wwwwx	www--
1410-1430 (ammonium)	wwwww	wwwww	wwwww	wwwwx	wwwwx	www--
1730-1740 (carbonyl)	waaax	waaax	aaaax	waxax	waaax	wax--
865-885 (organosulfur)	xaaax	xaxxx	xaaax	xxxxx	xaaax	xxx--
540, 1035 (soil dust)	ppxxx	ppxxx	ppxxx	ppxxx	ppxxx	ppx--

^a Results of solvent rinses conducted on samples collected from August 13-24. Unless otherwise indicated, samples were analyzed, then rinsed in hexane, acetone, and water. Spectra were collected after each rinse. Samples were collected from 0700-1900 EDT on both dates listed. Table entries describe whether an absorbance in the range shown to the left was present and removed in the hexane, acetone, or water rinse. There were five samples for each sample date. An asterisk (*) indicates samples collected on these dates were rinsed only in acetone and water.

code	stage
p present	3 1.0-2.0 μm particles
h removed in hexane	4 0.5-1.0 μm particles
a removed in acetone	5 0.26-0.5 μm particles
w removed in water	6 0.12-0.26 μm particles
p present and not removed	8 0.05-0.12 μm particles
x below limits of detection	
- no rinse data	

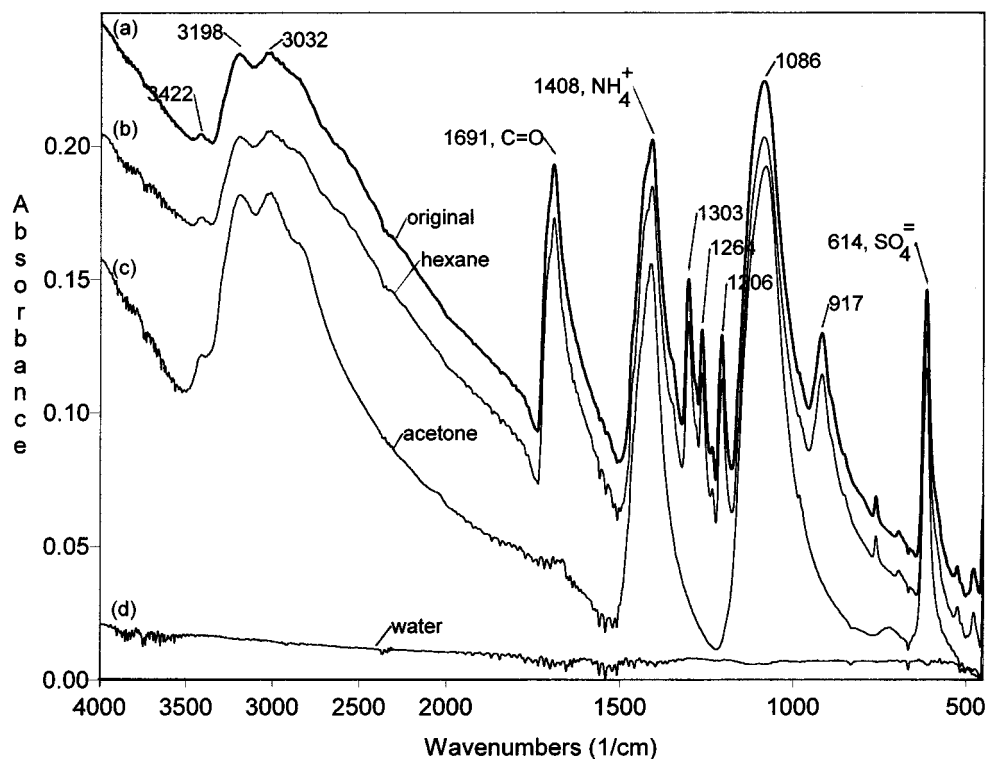


FIGURE 8. Spectra of a laboratory-generated glutaric acid and ammonium sulfate aerosol. Shown are the original spectrum (a), the spectrum after removing nonpolar organics with hexane (b), the spectrum after subsequent removal of polar organics in acetone (c), and the spectrum after subsequent removal of inorganic salts in water (d). Several absorbances are labeled with absorbance bands in wavenumbers. Note that sulfate (614 cm^{-1}) and ammonium (1406, 3032, and 3198 cm^{-1}) are removed in the water rinse. Carbonyl (1691 cm^{-1}) and other organic absorbances are removed in the acetone rinse.

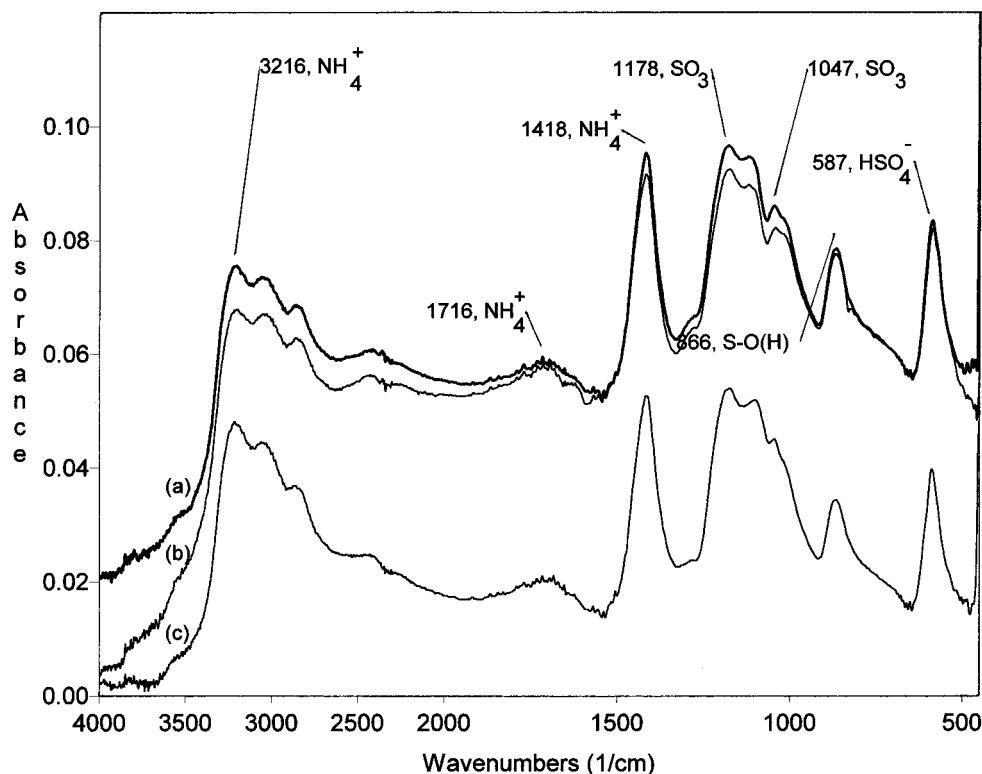


FIGURE 9. Spectra of ammonium bisulfate aerosol. Shown are the original spectrum (a), the spectrum after the hexane rinse (b), and the spectrum after the acetone rinse (c). The spectrum after the subsequent water rinse is not shown. Several absorbances are labeled with absorbance bands in wavenumbers. Note that bisulfate and ammonium absorbances are not removed in acetone.

associated with clay-like soil dust were found in the 1.0–2.0- μm diameter size fraction on all days for which solvent rinses were performed.

For contrast, the aliphatic section of a sample collected in a cigarette smoke-impacted residence is shown in Figure 7. This aerosol, which is expected to have substantial nonpolar organic constituents, has large aliphatic absorbances that are removed in hexane (34). This comparison provides confidence in the solvent rinse method as a means of evaluating the polarity of organic constituents.

Solvent rinses were also performed on laboratory-generated aerosols and blank ZnSe substrates. Both ammonium bisulfate aerosol samples and mixtures of ammonium sulfate and a single carbonyl-containing compound (i.e., oxalic, citric, tartaric, glutaric, and adipic acid) were generated and rinsed in the same manner as SEAVS samples. Neither sulfate nor bisulfate absorbances were removed in acetone, but these absorbances were completely removed in the water rinse as shown in the glutaric acid/ammonium sulfate spectrum of Figure 8 and ammonium bisulfate spectrum of Figure 9. Organic absorbances from glutaric and adipic acid were removed in the acetone rinse (Figure 8), whereas oxalic, citric, and tartaric acid absorbances were not removed until the water rinse. In SEAVS samples submicron carbonyl was removed in the acetone rinse, suggesting that Smoky Mountain submicron carbonyl compounds behave more like glutaric and adipic acid than they do like oxalic, citric, and tartaric acid. Ten blank ZnSe substrates rinsed sequentially with solvents had no detectable absorbances. Several dynamic blanks were also collected by sampling the output of the aerosol generation system when only deionized water was atomized. Resulting samples had no artifactual absorbances, indicating that the solvents and standard preparation system did not cause any contamination.

Organosulfur. The functional group(s) responsible for absorbances at approximately 875, 1045, 1225, and 2500 cm^{-1} (see Figure 5) are presumably associated with polar organics

because they were removed with acetone. Solvent rinses conducted on laboratory-generated aerosol samples verified that neither ammonium sulfate nor ammonium bisulfate were removed in the acetone rinse (Figure 9). Organonitrates have been observed in Los Angeles and are a product of photochemical oxidation with absorbances near 860 and 1280 cm^{-1} . However, the material removed in the acetone rinse has a spectrum that much more closely resembles the spectra of sulfur-containing organics. The asymmetric stretching of S–O–C (e.g., in organic sulfates) results in an absorbance at approximately 875 cm^{-1} . Symmetric and asymmetric stretchings of SO_3 , present in sulfonic acid salts, occur at 1030–1070 cm^{-1} and 1140–1280 cm^{-1} , respectively. An OH absorbance near 2500 cm^{-1} is present in hydrated sulfonic acids. In addition, peak splitting was observed on the three peaks located at 590, 865, and 1045 cm^{-1} , suggesting that peaks at 865 and 1045 cm^{-1} have some characteristics in common with the 590 cm^{-1} bisulfate peak. This also suggests that the compounds characterized by absorbances at approximately 875, 1045, 1225, and 2500 cm^{-1} are sulfur containing, and their removal in acetone suggests they are organic.

In the marine boundary layer, methane sulfonic acid is believed to be formed from the oxidation of dimethyl sulfide (35, 36). Alkyl and methane sulfonic acids and sulfonates have also been observed in polluted continental air masses and fogs (37–39). They are postulated to form in the gas phase from H_2SO_3 and either aldehydes or substituted aromatic hydrocarbons and in the aqueous phase from SO_2 -aldehyde reactions (37, 40–42). Camphorsulfonic acid, for example, has absorbances at 854, 1046, 1180, and 1280 cm^{-1} and a broad absorbance in the 2500–2600 cm^{-1} region. These spectral characteristics correspond roughly to the acetone-soluble absorbances we observed. A spectrum of camphorsulfonic acid is shown in Figure 10. Camphorsulfonic acid is soluble in acetone, and can be formed from camphor in the presence of aqueous acidic sulfate. Camphor is a tracer

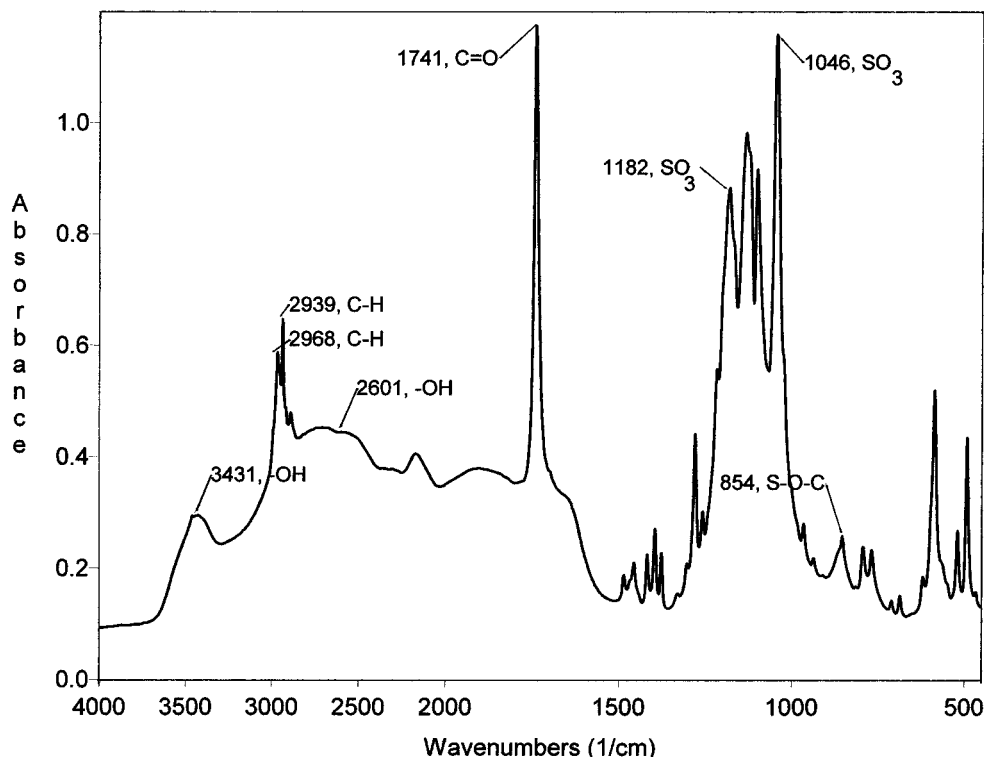


FIGURE 10. Spectrum of camphorsulfonic acid, provided here as an example of an organosulfur compound.

of biogenic emissions (31). Camphorsulfonic acid is not an exact match with SEAVS spectra, but its commonalities suggest that sulfonic acids are a plausible compound class. Other sulfur-containing polar organics that have been observed or are expected to form include benzothiazol (43), organic sulfates (44), cyclic organic sulfites (41), and dimethyl sulfite (41). It is not likely that organosulfur compounds account for a substantial fraction of total particulate sulfur. However, they could account for a significant portion of the organic aerosol in the Smoky Mountains.

Discussion

The polarity of the aerosol, the predominance of sulfate, carbonyl, and organosulfur absorbances, and the size distribution of carbonyl carbon suggest that secondary formation processes have a large influence on the concentration, composition, and size distribution of the fine aerosol in the Smoky Mountains. Direct FTIR analyses of substrates before and after solvent rinses enabled characterization of polar and nonpolar organics in samples much too small for traditional extraction and analysis. The spectral simplification the rinses provided was crucial to the identification of organosulfur compounds in the Smoky Mountain aerosol. These compounds could be a significant contributor to organic aerosol mass at Look Rock. Rinses also showed that the organic aerosol was mostly polar. The small nonpolar fraction of the fine aerosol ($<2.0 \mu\text{m}$) was likely the result of primary biogenic and geogenic emissions, such as plant waxes and windblown soil dust. Unimodal size distributions were observed for carbonyl carbon for all but two samples (August 3–4 and August 21–22). Distributions peaked between 0.26 and $1.0 \mu\text{m}$ in diameter. Carbonyl size distributions in the Smoky Mountain samples were distinctly different from the bimodal distributions observed in Los Angeles. Future work will include quantitation of carbonyl concentrations (i.e., response factor determination) and further examination of spectra and size distributions associated with sulfur-containing organics in the aerosol.

Acknowledgments

This research was supported in part by the Electric Power Research Institute (Contract W09116-02), the NIEHS Center of Excellence (ES 05022) at the Environmental and Occupational Health Sciences Institute, Rutgers Cooperative Extension and the New Jersey Agricultural Experiment Station. The use of size-resolved sulfate data collected by the University of Minnesota is gratefully acknowledged, as are discussions with James Eliot and David Allen, Lisa Zussman's management of the New Brunswick sampling site, and Martha Dunbar's assistance with substrate preparation. New Brunswick samples were collected at a site made available by Charlie Pietarinen, Chief of Air Monitoring at the New Jersey Department of Environmental Protection (DEP). The continued support of the DEP is much appreciated.

Literature Cited

- (1) Saxena, P.; Hildemann, L.; McMurry, P.; Seinfeld, J. J. *Geophys. Res.* **1995**, *100*, 18755–18770.
- (2) Wagner, J.; Andrew, E.; Larson, S. J. *Geophys. Res.* **1996**, *101*, 19533–19540.
- (3) Andrews, E.; Larson, S. M. *Environ. Sci. Technol.* **1993**, *27*, 857–865.
- (4) Gill, P.; Graedel, T.; Weschler, C. *Rev. Geophys. Space Phys.* **1983**, *21*, 903–920.
- (5) Lioy, P.; Daisey, J.; Atherholt, T.; Bozzelli, J.; Darack, F.; Fisher, R.; Greenberg, A.; Harkov, R.; Kebbekus, B.; Kneip, T.; Louis, J. J. *Air Pollut. Control Assoc.* **1983**, *33*, 649–657.
- (6) Matsumoto, H.; Inoue, K. *Arch. Environ. Contam. Toxicol.* **1987**, *16*, 409–416.
- (7) Gray, H. A.; Cass, G. R.; Huntzicker, J. J.; Heyerdahl, E. K.; Rau, J. A. *Environ. Sci. Technol.* **1986**, *20*, 580–582.
- (8) Shah, J. J.; Johnson, R. L.; Heyerdahl, E. K.; Huntzicker, J. J. *Air Pollut. Control Assoc.* **1986**, *36*, 254–257.
- (9) Vasconcelos, L. A.; Macias, E. S.; White, W. H. *Atmos. Environ.* **1994**, *28*, 3679–3691.
- (10) Lioy, P. J.; Daisey, J. *Environ. Sci. Technol.* **1986**, *20*, 8–14.
- (11) Rogge, W. F.; Mazurek, M. A.; Hildemann, L. M.; Cass, G. R. *Atmos. Environ.* **1993**, *27*, 1309–1330.
- (12) Kawamura, K.; Kasukabe, H.; Barrie, L. *Atmos. Environ.* **1996**, *30*, 1709–1722.
- (13) Khwaja, H. *Atmos. Environ.* **1995**, *29*, 127–139.

- (14) Pankow, J. F. *Atmos. Environ.* **1987**, *21*, 2275–2283.
- (15) Pankow, J. F. *Atmos. Environ.* **1994**, *28*, 185–188.
- (16) Pickle, T.; Allen, D. T.; Pratsinis, S. E. *Atmos. Environ.* **1990**, *24A*, 2221–2228.
- (17) Mylonas, D. T.; Allen, D. T.; Ehrman, S. H.; Pratsinis, S. E. *Atmos. Environ.* **1991**, *25A*, 2855–2861.
- (18) Palen, E. J.; Allen, D. T.; Pandis, S. N.; Paulson, S.; Seinfeld, J. H.; Flagan, R. C. *Atmos. Environ.* **1993**, *27A*, 1471–1477.
- (19) Gundel, L.; Daisey, J.; Carvalho, L. D.; Kado, N.; Schuetzle, D. *Environ. Sci. Technol.* **1993**, *27*, 2112–2119.
- (20) Grader, G. S.; Flagan, R. C.; Seinfeld, J. H.; Arnold, S. *Rev. Sci. Instrum.* **1987**, *58*, 584–587.
- (21) Gordon, R.; Trivedi, N.; Singh, B. *Environ. Sci. Technol.* **1988**, *22*, 672.
- (22) Junkermann, W.; Ibusuki, T. *Atmos. Environ.* **1992**, *26A*, 3099–3103.
- (23) Vogt, R.; Finlayson - Pitts, B. *J. Phys. Chem.* **1994**, *98*, 3747–3755.
- (24) Vogt, R.; Elliott, C.; Allen, H.; Laux, J.; Hemminger, J.; Finlayson-Pitts, B. *Atmos. Environ.* **1996**, *30*, 1729–1737.
- (25) Saxena, P.; Musarra, S. Report to Electric Power Research Institute, 3412 Hillveiw Ave. Palo Alto, CA 94303, 1997.
- (26) Hering, S. V.; Flagan, R.; Friedlander, S. *Environ. Sci. Technol.* **1978**, *12*, 667–673.
- (27) Hering, S. V.; Friedlander, S.; Collins, J.; Richards, L. *Environ. Sci. Technol.* **1979**, *13*, 184–188.
- (28) Allen, D. T.; Pallen, E. J.; Haimov, M. I.; Hering, S. V.; Young, J. R. *Aerosol Sci. Technol.* **1994**, *21*, 325–342.
- (29) Liu, L.; Burton, R.; Wilson, W. E.; Koutrakis, P. *Atmos. Environ.* **1996**, *30*, 1237–1245.
- (30) Liou, P. J.; Samson, P. J.; Tanner, R. L.; Leaderer, B. P.; Minnich, T.; Lyons, W. *Atmos. Environ.* **1980**, *14*, 1391–1407.
- (31) Mazurek, M. A.; Cass, G. R.; Simoneit, B. R. T. *Environ. Sci. Technol.* **1991**, *25*, 684–694.
- (32) Grosjean, D.; Friedlander, S. K. *J. Air Pollut. Control Assoc.* **1975**, *25*, 1038–1044.
- (33) van der Marel, H. W.; Beutelspacher, H. *Atlas of Infrared Spectroscopy of Clay Minerals and Their Admixtures*; Elsevier: New York, 1976; p 57.
- (34) Carlton, A. G.; Johnson, W.; Buckley, B.; Simick, M.; Eisenreich, S.; Turpin, B. J. Tools for Characterization of Personal Aerosol Exposures *Aerosol Sci. Technol.* **1998**, manuscript in preparation.
- (35) Ayers, G. P.; Gras, J. L. *Nature* **1991**, *353*, 834–835.
- (36) Kreidenweis, S. M.; Penner, J. E.; Yin, F.; Seinfeld, J. H. *Atmos. Environ.* **1991**, *25A*, 2501–2511.
- (37) Panter, R.; Penzhorn, R. D. *Atmos. Environ.* **1980**, *14*, 149–151.
- (38) Munger, J. W.; Jacob, D. J.; Hoffmann, M. R. *J. Atmos. Chem.* **1984**, *1*, 335–350.
- (39) Jacob, D. J.; Gottlieb, E. W.; Prather, M. J. *J. Geophys. Res.* **1989**, *91D*, 2801–2804.
- (40) Dasgupta, P. K.; DeCesare, K. B.; Brummer, M. *Atmos. Environ.* **1982**, *16*, 917–927.
- (41) Eatough, D. J.; Hanson, L. D. *Adv. Environ. Sci. Technol.* **1983**, *12*, 221–268.
- (42) Olson, T. M.; Hoffmann, M. R. *Atmos. Environ.* **1989**, *23*, 985–997.
- (43) Dong, M. W.; Locke, D. C.; Hoffmann, D. *Environ. Sci. Technol.* **1977**, *11*, 612.
- (44) Roberts, J. D.; Caerio, M. E. In *Basic Principles of Organic Chemistry*; W. A. Benjamin Inc.: New York City, 1964; p 175.

Received for review May 9, 1997. Revised manuscript received December 1, 1997. Accepted December 11, 1997.

ES970405S